APPLICATION

Heat transfer simulation and improvement of autoclave loading in composites manufacturing

Shokoufeh Mirzaei[1] · Krishna Krishnan[2] · Charbel Al Kobtawy[1] · Jeffrey Roberts[1] · Eric Palmer[1]

Abstract

Composite manufacturing has proven to be a quintessential process for the improvement of a spectrum of industries from medical to automotive, and aerospace. Most composite manufacturing processes include a two-step process, lay-up, and autoclave curing. The autoclave process is often long and expensive. Therefore, improving its efficiency can reduce the production cost and increase the throughput significantly. However, there is a scarcity of studies in the literature that tackle production improvement of vacuum bag/autoclave molding processes. Thus, in this paper, in collaboration with an industry partner, the effect of quantity, location, and orientation of parts inside an autoclave on the curing cycle is investigated both computationally and experimentally. The objective is to improve the production rate without compromising quality. The quality of parts is being represented by their heat-up rate throughout the curing cycle. The results showed that, for a specific scenario, doubling the number of parts inside the autoclave could slow down the heat transfer without significantly affecting the heat-up rates. As a result, the lag could be negligible for the increase in the production rate that it provides.

Keywords Composites manufacturing · Autoclave curing cycle · Numerical simulation · Design of experiments

1 Introduction

Composite materials usually have unique properties, the most significant of which is the high strength-to-weight ratio. The incorporation of composite parts in the aerospace industry has permitted increased speed, improved fuel efficiencies by reducing part weight, and increased reliability by increasing strength and durability. Composite materials consist of two or more types of individual components. This combination is generally implemented to realize the benefits of each component individually while achieving a new material that is superior in performance to each of the composite individual parts.

One of the most widely used techniques for composite manufacturing is the vacuum bag/autoclave molding process, which involves placing resin and fibers in a mold enclosed in a vacuum bag. This process involves the lay-up of a variety of layers to form an assembly. Once assembled, the vacuum bags are inserted in an autoclave. Inside the autoclave, a vacuum is created, which forces out air and any excess resin. This process will compact the vacuum bag, which will then be subjected to high temperature and pressure, causing the laminate to consolidate. The entire process inside the autoclave is called a curing cycle. More specifically, the curing cycle consists of a heat-up or ramp-up period, dwell time, and a cooling period. During the heat-up period, the parts are expected to reach a predetermined curing temperature. Once the curing temperature is reached, the parts are maintained at the dwell temperature for a given duration, which varies depending on the part specifications. The dwell period begins after the coldest, lagging point of the parts within the autoclave reaches the curing temperature. Constant high pressure is maintained throughout the process until the cooldown period begins.

The effect of variation of curing parameters on the quality of composite materials has been extensively studied in the literature [1–17]. In these studies, one or two curing parameters were changed to intentionally induced various defects in

✉ Shokoufeh Mirzaei
  smirzaei@cpp.edu

[1] Industrial and Manufacturing Engineering Department, California State Polytechnic University, 3801 W Temple Ave, Pomona, CA 91768, USA

[2] Industrial, Systems, and Manufacturing Engineering Department, Wichita State University, Wichita, KS, USA

the composite parts. Then, the correlation between the mechanical properties of interest and variation of the curing parameters was investigated. Some of these studies explored the effect of variations in curing temperature [1–4], pressure [7–13], or both [17] on the mechanical properties of composite parts. While others investigated the design of proper curing cycles to improve the mechanical properties of composite parts [5, 6, 18]. There are also studies investigating the design optimization of autoclave molds to improve curing quality and performance of composite [19, 20].

In addition to pressure and temperature, a change in the loading of an autoclave, which means the different placement of parts and/or different numbers of loaded parts, leads to different airflow patterns that can affect the curing cycle [21]. Slesinger [22] experimentally showed that changing the parts' locations inside the autoclave will significantly affect the heat transfer coefficient (HTC). Bohne et al. [23] numerically and experimentally studied the relation between HTC and the location of parts inside the autoclave. They found that a part placed in the front region of the autoclave, where air velocity is the highest, could have an HTC twice as large as the HTC of a tool placed in the rear of the autoclave where the air is slower. Some researchers argued that the incidence angle in which the hot air reaches a plate has a significant effect on the heat transfer to the plate, whether it is a composite material in an autoclave or an urban building. Sturrock [24] studied the effect of wind direction on convective heat transfer by placing cube-shaped building models in a wind tunnel. He found that the highest HTC occurred with an incidence angle of 30°. In contrast, early research by Rowley [25] found no significance in the effect of flow direction by studying flow angles between 15 and 90° to the surface.

Heat transfer is a major contributing factor during the curing process of composite materials. It generally occurs in 3 forms:

1. Forced convection between the solid and the moving hot gas.
2. Conduction between the different layers of the part.
3. Heat production by the polymerization reaction through the thickness of the part.

The entire heat transfer mechanism is regulated by forced convection. While the literature is extensive in investigating the effect of pressure and temperature changes on the curing cycle, it is very sparse on the impact of autoclave loading on curing cycles, especially when forced convection used for modeling the heat transfer. Additionally, in the literature concerning autoclave heat transfer, the main objective of efficient curing cycles, which is curing the maximum number of parts in the shortest possible time, is often neglected. For example, it is not clear when the number of parts is doubled (two racks), how it will affect the curing cycle and whether it

is worth the 100% increase in production rate, and whether it will maintain the product quality. Therefore, the main contribution of this paper is to investigate the effect of autoclave loading and its variation on (1) the curing cycle; (2) the heat-up rate of parts as a measure of their quality and acceptance.

In sections 2 and 3 of this paper, we will explain the computational and experimental methods of our study. In section 4, we summarize the results and findings, explaining the assumptions and limitations of the study as well as avenues for further research.

2 Computational study

2.1 The autoclave

For this study, the curing process occurs in a specific autoclave to reduce outside noise and variabilities not otherwise associated with the control parameters of the study. The autoclave chosen for the study is modeled after an existing one at a partner company. It is a cylindrical model with a blower located at the rear, which blows hot gas through a metal sheet annulus. The annulus forms a 2.5″ conduit with the boundaries of the autoclave. The gas circulates through this opening until it reaches the front of the autoclave, where the flow reverses once it hits the curved door. The gas then travels back through the center and exits the chamber through a radiator that cools down the gas before it is heated up again and blown back inside the 2.5″ opening. The autoclave has an interior diameter of 6′, measured to the interior surface of the metal sheet annulus. The interior length, from the lip with the door open to the cooling radiator located at the rear, is 12′. The door's interior has a hybrid shape, which is comprised of both flat and curved surfaces. The operating conditions are at 425 °F and 125 PSI. When facing the door, on the left side, there are ten vacuum source ports spread along the length of the autoclave; on the opposite side, are ten vacuum monitor ports. Each part requires a minimum of 1 vacuum source and one monitoring port. The operating gas inside the autoclave is nitrogen. We used a representative prism to physically and thermally represent actual molds, also known as tools, inside the autoclave. The representative prisms were chosen to represent parts as large as 6.5″ × 6.5″ × 18″.

One of the major problems of the curing cycle is that a portion of composite parts does not remain within the required specifications. More specifically, the lagging or trailing edge of the part is not maintaining the minimum ramp rate required. While this is problematic on the trailing edge of the parts, the issue is not present on the leading edge. The ramp rate varies based upon the given temperature. According to parts' specifications, parts need to maintain a defined ramp rate at various points during the process over a given average time frame. Table 1 shows an example of the required ramp rates for a part:

Table 1 An example of the required ramp rates for a part

Temp	Ramp rate spec requirement
Ambient–54 °C	No requirement
54–88 °C	1.11 °C/min–4.44 °C/min
88–110 °C	0.56 °C/min–4.44 °C/min
110–120 °C	0.17 °C/min–4.44 °C/min
120-dwell temp	No requirement (must dwell at 127±5 deg for 100 mins)

Table 1 shows that the ramp rate remains constant at 4.44 °C/min throughout the process, while the minimum ramp rate begins at 1.11 °C/min and reduces as the temperature increases, this can be seen in Fig. 1. Figure 1 shows the temperature vs. ramp rate graph, with the mean observed ramp rate depicted as a black dashed line located slightly above the minimum required ramp rate throughout the process.

One major issue of composite manufacturing is that the specifications are not met consistently on the trailing edge of parts. If the 10-min average ramp rate of any part falls outside of the specification for any portion, the part is rejected. Inside an autoclave, the temperature is monitored through various thermocouples located across the surface of each part. Often the autoclave process temperature ramp rate is set to the maximum ramp rate, i.e., the autoclave is not capable of ramping up the temperature at a higher rate than current operation.

The purpose of the simulation is to investigate the heat profile and spacing of a particular prism in the model autoclave to reduce the number of rejected parts and to improve the curing cycles in order to increase the number of parts cured at once.

2.2 Simulation model

In this study, we used computational fluid dynamics (CFD) simulation to model the heat transfer inside the autoclave described in section 2.1, which is loaded with parts. The main purpose is to test the possibility of increasing the number of loaded parts during a single run while maintaining the heat-up rates within the acceptable limits and minimizing total cure cycle times. To this end, different scenarios were numerically simulated using ANSYS Fluent software. The scenarios are chosen to allow a comprehensive analysis of how the number of loaded parts, their placement, and orientation affect the heat transfer inside the autoclave. We attempted to establish a model that predicts how loading the autoclave can affect curing cycles each time.

Our simulation only models the heat-up process of the cure cycle. So, one of the outputs will be the time it takes the parts to reach the curing temperature. Because, the more time it takes a single part to reach the curing temperature, the slower the whole cycle becomes. Additionally, since all parts during the curing cycle must achieve certain predefined heat-up rates, other simulation outputs that will be calculated and analyzed are the heat-up rates. The heat transfer modeled in this study will be the forced convection from moving hot nitrogen to the molds. The conduction through the different layers of materials is ignored in this paper. Mainly because the convective heat transfer initiates and regulates the total heat transfer mechanism inside the autoclave and thus its simulation gives us a clear idea of the total heat transfer behavior and will form a solid understating of the objectives defined in this research. As a result, the temperature change on the surface of the molds is of most interest and will be used to draw results and conclusions.

2.2.1 Operating conditions

For the different simulation scenarios, the variable parameters were the position of the molds, the number of the molds, and their orientation inside the autoclave. Also, the operating conditions inside the autoclave remained the same for all

Fig. 1 Temp vs. ramp rate graph
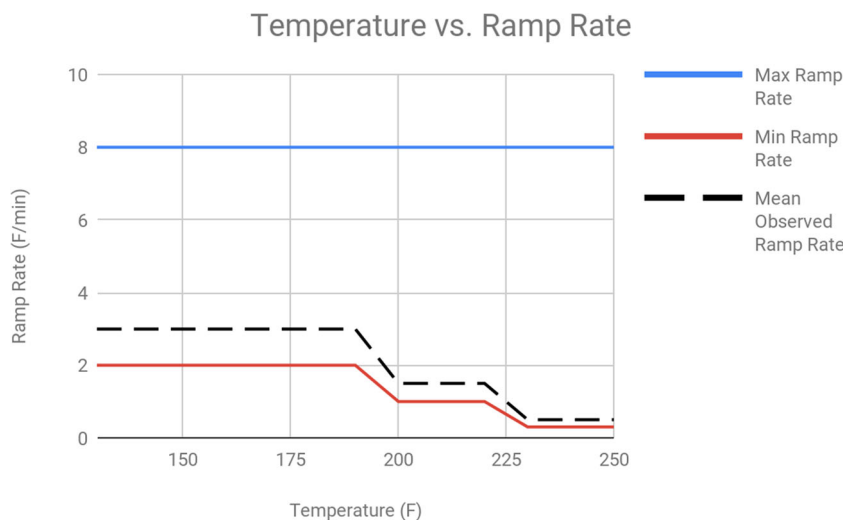
scenarios. To replicate the real behavior of the autoclave and molds during the curing cycles in real-life, the conditions inside the simulated autoclave had to be the same as those used during actual cycles. The real autoclave conditions were modeled after a common autoclave model owned by a partner company. The benchmark autoclave is pressurized to 90 PSI. The vacuum is vented when the pressure reaches 15 PSI. The temperature of the air for every time step increases from ambient temperature to a maximum of 250 ± 10 °F before it cools down. The dwell time at the maximum temperature is 100 min. The cycle duration to cure 2 to 3 parts is approximately 5 hours. The only unknown parameter of the benchmarked autoclave was the velocity of the nitrogen gas inside the autoclave. The absence of blower specifications hindered gathering velocity data. Therefore, the velocity at the inlet of the autoclave was measured experimentally for simulation purposes. Since it was impossible to access the back of the autoclave, the velocity was measured at the exit of the metal sheet annulus near the door at atmospheric pressure and temperature, and with the door of the autoclave open. The average velocity was found to be 5 m/s. As a result, the conduit in which the gas flows between the annulus and the boundaries of the autoclave was omitted from the simulation to simplify the geometry, since the simulation started at the exit of that conduit.

2.2.2 Parameter settings

Figure 2 shows the model of the autoclave used for the simulation as well as the chosen inlet and outlet positions. The autoclave's actual dimensions were maintained. The mold chosen for the simulation was a prism with the following dimensions: $6.5'' \times 6.5'' \times 18''$. Simulating one type of mold will exclude the effects of variation in mold's dimensions during the experiments. Initial testing of the empty autoclave was conducted in steady-state mode to make sure that the gas
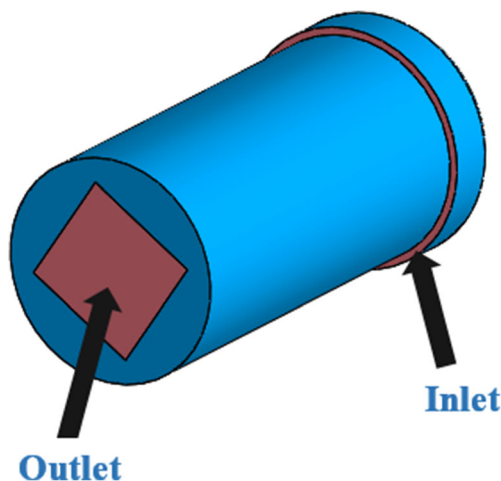

Fig. 2 Autoclave inlet and outlet locations

flow follows the general pattern, which is reflected at the door and returns through the center to the exit through the radiator.

To simulate the heat transfer inside the autoclave, a transient model was used as the problem is time-dependent. At all times and for all scenarios, the mesh was drawn with the highest possible resolution to ensure the adequate convergence of the problem. The maximum allowed number of elements was 512,000. In terms of boundary conditions, inserting a pressure of 90 PSI at the inlet and outlet ensured that the pressure remained constant throughout the cycle. At the inlet, the velocity of 5 m/s could not be considered as representative of the actual velocity inside the autoclave at a pressure of 90 PSI (which is more than 6 times the atmospheric pressure) and a temperature of 250 F, as it resulted in a very slow heat transfer. Therefore, this velocity was used as an initial setpoint, and different experiments with inlet velocities were conducted. Finally, an inlet velocity of 25 m/s, showed comparable results with the real numbers provided by the partner company. As for the temperature, a transient inlet boundary condition was selected using the data for the gas temperature variation with time from the partner's company cure reports. When the inlet temperature reaches 250 ± 10 °F, it is held at this value until all the molds reached that temperature. In the beginning, the temperature of the molds was set to the atmospheric temperature of 66 F.

The actual curing cycles are very time consuming, and the heat-up period during actual parts curing alone could take up to 3 h. A time step of 1 s was chosen for the first minute that the flow progresses, then it was raised to 5 s for another 10–15 min, while the remaining was computed with a time step of 10 s. These large time steps affected the convergence but were a reasonable compromise to achieve a more practical computation time. For all simulation scenarios, the temperature was monitored for every mold inside the autoclave. More specifically, the minimum temperature, the average surface temperature, and the average volume temperature were measured. It was very crucial to also generate data about the velocity of the flowing hot nitrogen, as well as other data such as pressure inside the autoclave.

2.2.3 Description of scenarios

Each scenario that was simulated required a different placement of molds inside the autoclave and/or different numbers of molds. The autoclave-mold configurations for each scenario are as follows:

Scenario 1: Simulation of 4 molds along the length of the autoclave Four molds were placed inside the autoclave. They were placed in the center of the autoclave radially but spread apart along the length of the autoclave following the z coordinate (horizontal line). The nearest to the front was 20″ from the lip of the door, and all the molds were then 20″ apart. This clearance offers a manipulatable distance between 2

consecutive parts. This scenario was run three times to generate three sets of results.

Scenario 2: Simulation of 2 levels of 4 molds each All the molds were placed in the z-direction the same way as scenario 1 for both levels. However, radially along the y-axis (vertical), the distance between the closest extremities of the molds, top side of the bottom level and bottom side of the top level, was a practical 14″ distance. This scenario was also run three times to generate three sets of results. The placement of the molds inside the autoclave for scenarios 1 and 2 is shown in Fig. 3.

Scenario 3: Simulation of 4 molds rotated at 45° around the vertical axis The same model from scenario 1 was used here. However, all the molds were rotated to the right, around the vertical y-axis, by 45°.

Scenario 4: Simulation of 8 molds rotated at 45° around the vertical axis The same model from scenario 2 was used here. However, all the molds were rotated to the right, around the vertical y-axis, by 45°.

2.2.4 Simulation results and discussions

The variable of interest was the temperature of the molds at every step of flow time since this was a heat transfer simulation. Similar to the literature review, the lagging point inside the autoclave during the cure cycle is the most important point, since it initiates the remaining steps of the cycle. For this reason, in the rest of this section, the temperature that will
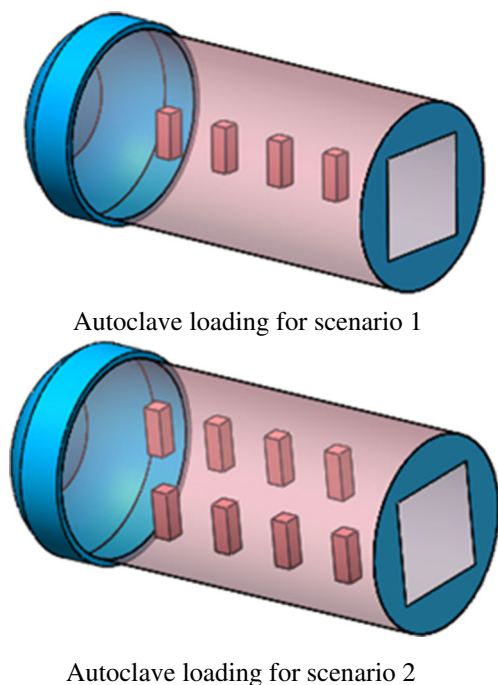

Autoclave loading for scenario 1

Autoclave loading for scenario 2

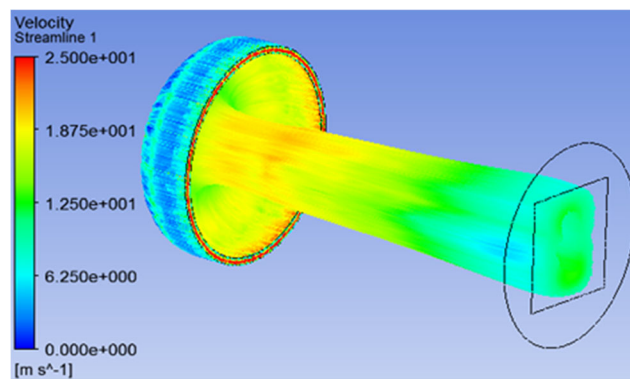**Fig. 3** Autoclave loading for scenarios 1 and 2

Fig. 4 Streamlines of nitrogen flow for the base model

be looked at and used in compiling the results and analysis is the minimum temperature or the trailing edge on the surface of every mold.

Scenario 1, which consisted of simulating 4 molds spread from the front to the back of the autoclave, will be considered as the base model of the study and will be compared with all other scenarios. This strategy will help discover the answers to the constraints of autoclave loading and attain the purpose of this study. The flow of hot nitrogen inside the autoclave is shown in Fig. 4. It can be seen that the gas follows the curvature of the door and return inside to the back of the autoclave where it exits through the radiator. The velocity of the gas decreases as it reaches the outlet. Radially, the velocity is maximum at the center of the autoclave, and decreases when moving up or down, or left or right. As for the temperature, we studied the temperature rises of the leading point in the autoclave from the simulation results versus the temperature rise of one of the thermocouples during an actual cure cycle made by the partner company. The results showed that although the simulated molds slightly lag behind the actual parts, as shown in Fig. 5, it is a good estimation of the real thermal behavior of the molds.
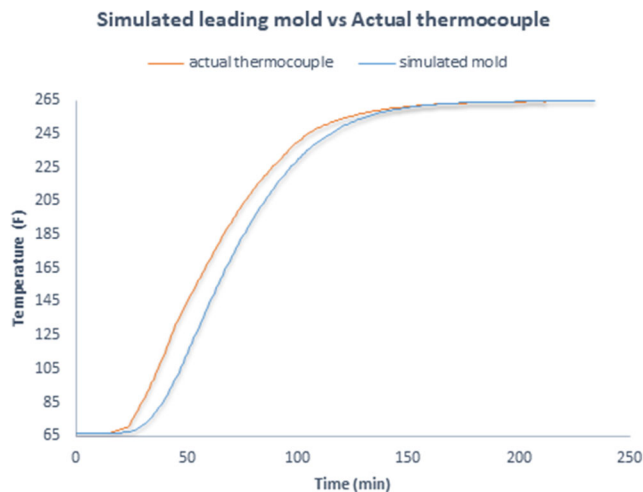

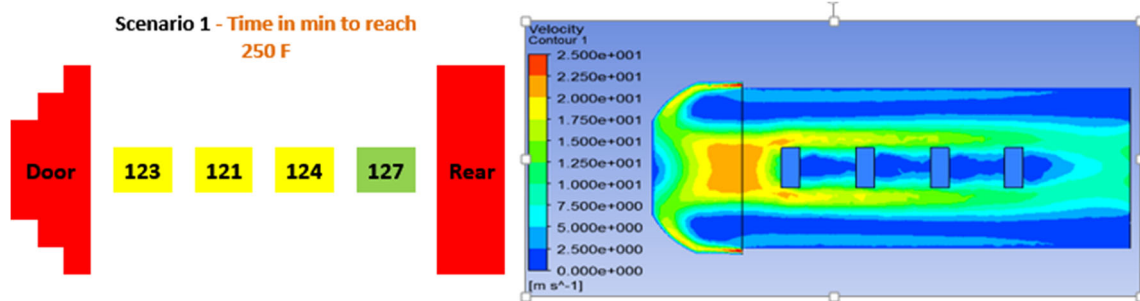**Fig. 5** Heat profiles of the simulated leading mold vs. an actual thermocouple

Fig. 6 Time in min to reach 250 °F for scenario 1 (left) and velocity contour for scenario 1 (right)

To understand the effects of the proposed part-loading mechanisms on the heat up of the molds and the cure cycle, the base model will be compared with scenario 2 in what is called case 1. In case 2, the base model will be compared to scenario 3, to study the effects of molds' rotation by 45° on the heat up. Finally, case 3 will compare the base model to scenario 4, to look at the combined effect of increasing the number of molds and changing their orientation inside the autoclave.

Case 1 Since the curing cycle will not progress until the lagging point in the autoclave reaches the cure temperature, diagrams 1 and 2 in Fig. 6 and Fig. 7 on the left respectively show the corresponding time in minutes it takes each loaded mold to reach the cure temperature of 250 °F for scenarios 1 and 2. The lagging mold in each scenario is in green, and the rest are yellow. It can be seen that the heat up of the whole system becomes slower when the number of loaded molds doubles. This hypothesis can be confirmed with a 95% level of confidence. In fact, by looking at the velocity contours in Fig. 6 and Fig. 7, it can be seen that from scenarios 1 to 2, the molds move from an area of high velocity in the middle of the autoclave to an area of lower velocity. Also, only one side of the molds is exposed to hot and fast nitrogen gas. Generally, this condition should decrease the heat transfer coefficient (HTC) in scenario 2. What is surprising is that the lagging mold in scenario 2 is the nearest to the door, on the lower level. Looking at the velocity contours, one would expect the lagging mold to be one of the molds near the rear of the autoclave.

Case 2 Here also, the diagram in Fig. 8 on the left shows the time in minutes for the molds to reach 250 F. Rotating the molds by 45° will slow down the heat up of the molds, more significantly for the lagging mold near the rear of the autoclave. The decrease in heat transfer is very low and the added lag is only 4 min. By looking at the velocity contours in Fig. 8 on the right, it can be seen that the dynamics of the flow changes slightly, especially for the most right mold. In addition, the area of 0 to low velocity between the 2 right-sided molds grows from scenario 1 to scenario 3.

Case 3 This case had the purpose of showing the combined effect of loading more parts inside the autoclave, rotated at 45°. The diagram in Fig. 9 on the left clearly shows that the results from scenarios 2 and 3 add up to deliver the slowest heat transfer to the molds between all studied scenarios, as expected. The time to reach 250 °F reaches 140 min for 5 out of 8 molds. The added lag is 18 min. The velocity contours in Fig. 9 on the right show the change in flow dynamics which caused this decrease in heat transfer. The contour for scenario 4 shows that the lagging mold, which is near the rear of the autoclave on the upper level, for the most part, is in a region of gas velocity between 0 and 2 m/s. This suggests that this region must have recorded the lowest HTC.

To better present the differences between the compared mold-loading configurations, Fig. 10 shows a heat-up graph associated with each case discussed earlier. Each graph in the figure contains the fastest and slowest heat-up curves corresponding to the leading and lagging molds repectively. This method will display the full range of the heat-up for each case and will offer a different angle to look at the effects caused by
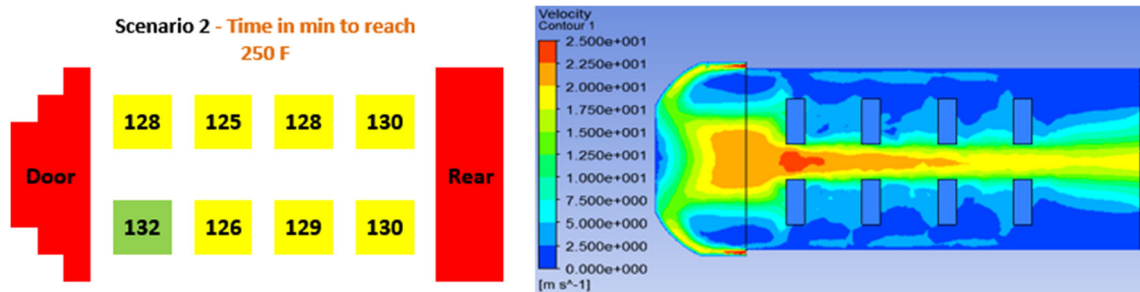

Fig. 7 Time in min to reach 250 °F for scenario 2 (left) and velocity contour for scenario 2 (right)
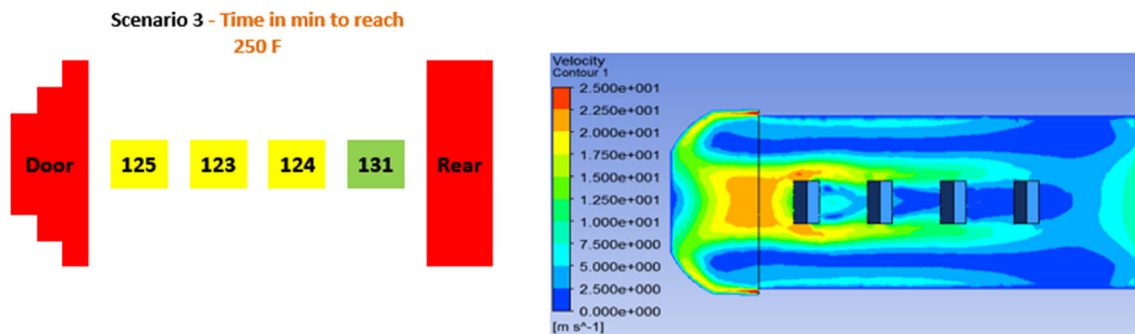
Fig. 8 Time in min to reach 250 °F for scenario 3 (left) and velocity contour for scenario 3 (right)

the variation in the loading type of the autoclaves. It is obvious that the biggest effect on the heat-up curves happens when the number of loaded molds in the autoclave doubled and rotated by 45°.

The results show that by adding a second level of molds inside the autoclave, or by rotating the molds by 45°, or by doing both, the heat-up of the molds slows down, which delays the total cure cycle. However, it slows it down by a relatively short amount of time, except for scenario 4.

Adding to this, the heat-up rates fall within the acceptable range for all scenarios. The results suggest that in all cases, it is better to keep the molds at an orientation where the gas flow hits the face of the molds, and not the edges. On the other hand, the results show that it is beneficial to add a second layer of molds inside the autoclave and to double the number of molds as the resulting delays are relatively short. It is more efficient to run the autoclave one time with 2 levels of molds and to experience a slight delay than to run the autoclave two times with 1 level of molds which double the cure cycle time. This method of manufacturing increases the production rate by 100% without adding a notable delay to the whole process.

For a one-level loading, it is always better to start loading from the front of the autoclave where the gas velocity is maximum (see scenarios 1 and 3). However, when 2 levels are used, there is not enough data to see if this method still stands. When the molds move out from the center gas stream, where velocity is maximum, it becomes harder to predict which location will be subject to the lowest HTC as seen in scenarios 2 and 4.

2.3 Production analysis

The current demand of the partner company for the selected part (represented by our prims) is 96 units per month.

Currently, the company loads a maximum of 3 parts in the autoclave per run. This production rate means that it takes 32 autoclave runs per month to meet the monthly demand. The time that it takes to complete a single run, from cure reports of 3 parts, is approximately 326 min. The time it takes the lagging thermocouple to reach 250 °F is 117 min.

According to the simulation results, by placing 8 parts for a single run in the autoclave, the heat-up rates fall within the acceptable range, there is enough space to fit eight parts, and there are enough vacuum ports for all 8. From the numerical simulations, the time it takes the lagging mold to reach 250 °F is 132 min (see scenario 2). As a result, the total time to complete a single run is going to be:

Total cure cycle for 8 parts per run = total cure cycle for 3 parts + lag difference.

= 326 + (132–117) = 341 min.

Also, the total number of monthly runs will be 96/8 = 12 runs. By loading eight parts together, the number of runs to achieve the production demand will go down from 32 to 12 runs.

The next step will consist of comparing the total curing time it takes per month to meet the current demand. This reduction in the number of runs results in 106 h reduction in total curing time per month.
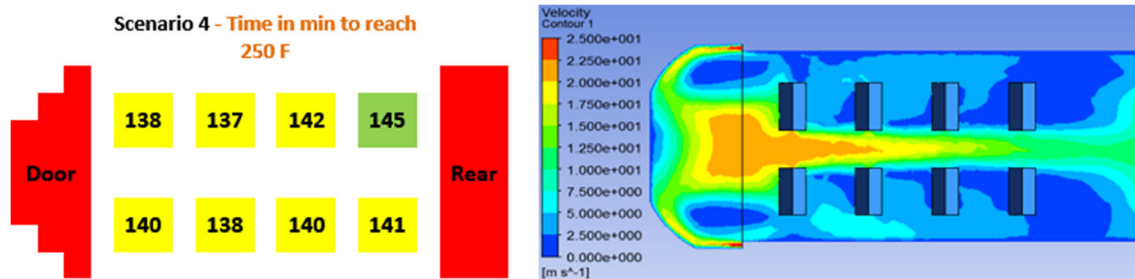

Fig. 9 Time in min to reach 250 °F for scenario 4 (left) and velocity contour for scenario 4 (right)
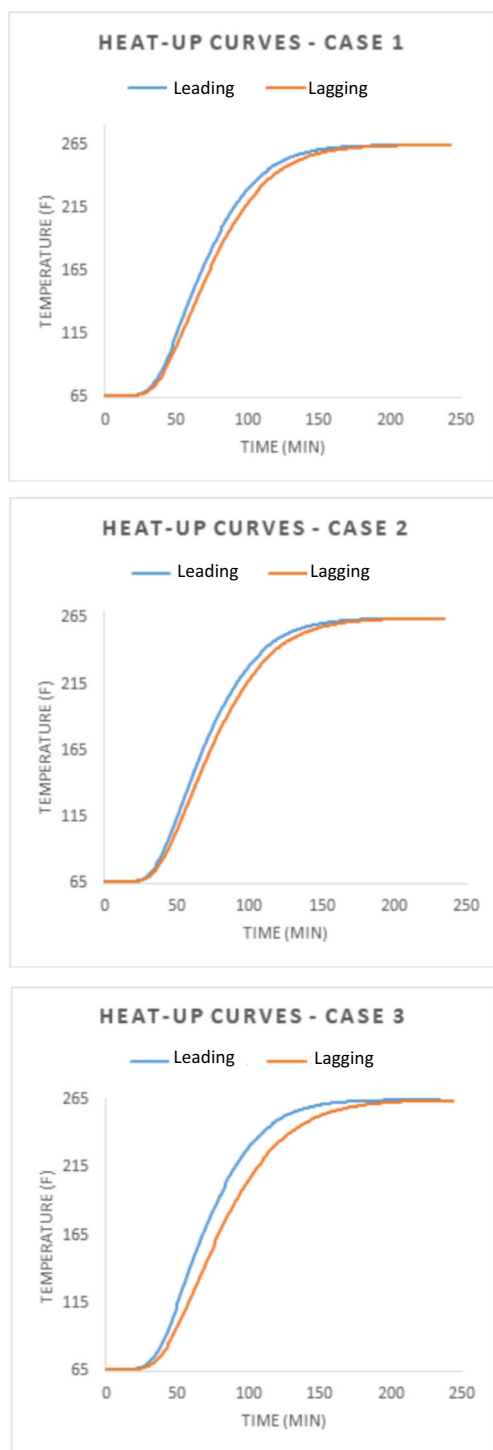
Fig. 10 Heat-up curves of leading vs lagging molds for case 1 (top), case 2 (center), and case 3 (bottom)

Table 2 shows the average heat-up rates calculated from the simulation results as well as those required by the partner company. The results of the numerical simulation suggest curing eight parts per single run. This will decrease the total cure cycle time to achieve a higher production rate per run.

Table 2 Comparing the heat-up rates calculated from the simulation results to the rates required by the partner company

		Heat-up rate			Required rates (F/min)
		Scenario 1	Scenario 2	Scenario 3	
Temperature range	130–190	2.55	2.44	2.23	2–8
	191–230	1.68	1.62	1.46	1–8
	231–250	0.88	0.84	0.74	0.3–8

The simulated model offers great insight into how the loading of the autoclave is going to affect the thermal behavior inside the autoclave with consideration of its limitations and assumptions.

In the next section, we propose a design of experiments to test the validity of the findings from the simulation model.

3 Design of experiments

In this section, we propose the application of design of experiments (DOE) to investigate the impact of rack location and level on the curing cycle. The metric chosen as the response value is the mean deviation. The mean deviation (MD) is the distance between the mean ramp rate for a given temperature range and the minimum ramp rate for that range, as shown in Eq. (1).

$$MD = \frac{\sum \left| RR_{avg} - RR_{\text{Lower}} \right|}{n} \qquad (1)$$

In Eq. 1, MD is the mean deviation, RR_{avg} is the average ramp rate of a given temperature range, and RR_{Lower} is the lower ramp rate threshold for that temperature range, and n is the number of measurements taken in that range. The MD is calculated over all sets of thermocouples (TCs) of an experiment, adjusted for each set of temperature ranges. A TC is a point temperature sensor for the scope of this study. Each part inside the autoclave was fitted with and assigned to 4 TCs, with temperature readings every minute. The TC assignments were as follows: two front and two aft the part, with two near the top while the other two located near the base of the part.

For the specific part and autoclave used in this study, there is no possibility of exceeding the maximum listed ramp rate of 8 °F/min. Therefore, we only need to be concerned with the lower threshold, which varies depending on the temperature range. Also, a 10-min averaged ramp rate below the minimum required rate would lead to part rejection. Thus, our objective is to maximize the MD.

To avoid interruptions in the current manufacturing schedule while implementing the experiments, inputs such as an
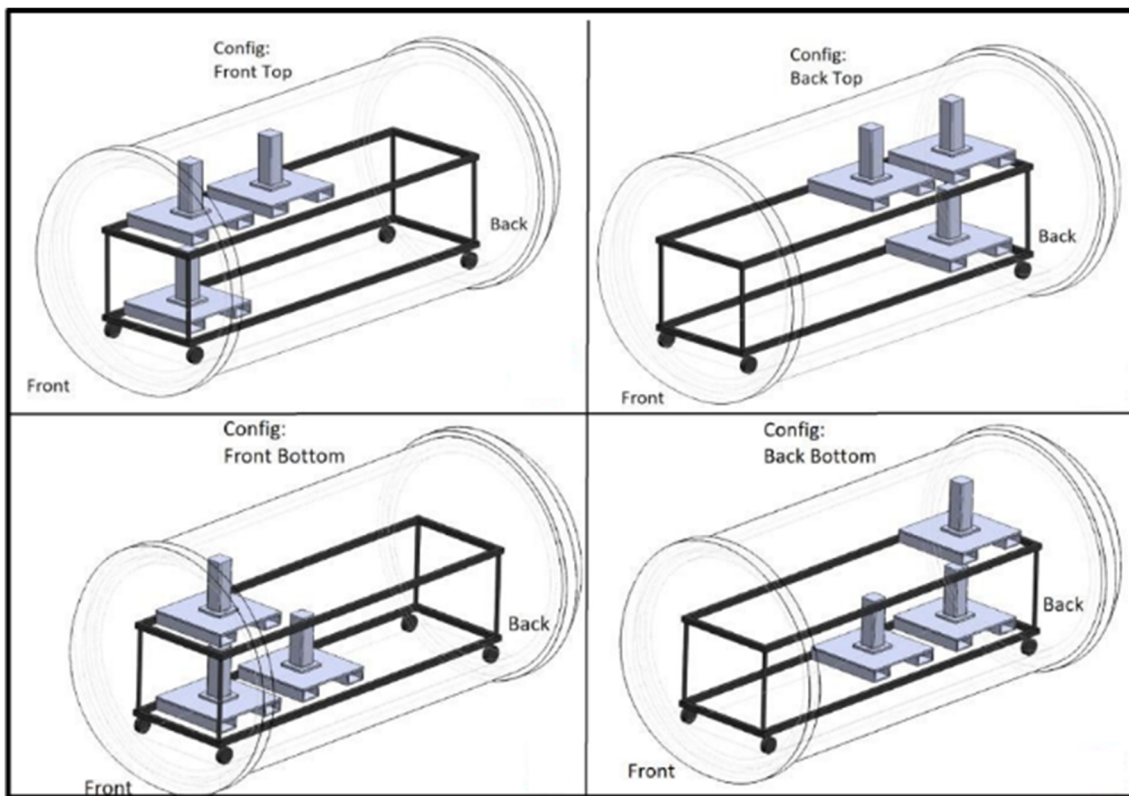
Fig. 11 Four tested configurations in the autoclave

increase in the number of parts in the autoclave or changing their orientation was not possible. These limitations, in combination with time constraints due to long batch processing times and downtimes, led to added limitations in designing and implementing the experiments. Therefore, the parameters considered for evaluation were the rack position and level. The rack position evaluates the position of parts in front or back of the autoclave. The front position is defined as the location with the closest proximity to the annulus, or hot air outlet, and the back position is the furthest from the air outlet. The rack level evaluates the level that parts are placed in the autoclave on the rack, either on the top of the rack or on the bottom.

Since only two parameters were available to test, we used a 2^2 Full-Factorial design. In a 2-factor Full-Factorial design, only four experiments are required to obtain data for testing the effect of parameters. Minitab 16 DOE tool was utilized to aid in experiments' setup and analysis.

Figure 11 shows the four tested scenarios or configurations: front top, front bottom, back top, and back bottom. Table 3 shows ramp regions assigned based on the temperature range.

Ambient–130 and 250–max ramp regions were outside the scope of the study, as no required ramp rates were assigned to these temperature ranges. Therefore, we only studied ramp regions 1, 2, and 3. The calculations of ramp rates were as follows:

$$RR_{avg} = \frac{\sum_1^{10} RR_t}{n} \qquad (2)$$

where RR_t is the ramp rate at time t,

$RR_t = \text{temp}_t - \text{temp}_{t-1}$. RR_{avg} is the 10-min average ramp rate. Then, the mean deviation was calculated using the MD given in Eq. (1). MD was calculated for each TC by ramp rate for a given temperature range. Each TC was associated with a part location given as front or back and top or bottom level, an average MD was taken of each location, and a summary was then derived producing a number which could be entered into Minitab for comparison of each experiment as shown in Table 4. The MD was selected as the value output from each experiment because of its nonbias property. From the lagging part thermocouple (PTC), ramp rates were observed in each tested configuration. It can be seen that the top front

Table 3 Ramp regions assigned based on the temperature range

Temperature (F)	Range
Ambient–130	Ramp region 0
130–190	Ramp region 1
190–230	Ramp region 2
230–250	Ramp region 3
250–max	Ramp region 4

Table 4 Data summary

		Average	Min	MD
Front bottom	Ramp 1	3.16	2.27	1.46
	Ramp 2	2.02	1.42	1.38
	Ramp 3	1.02	0.6	1.01
Back bottom	Ramp 1	3.14	2.33	1.14
	Ramp 2	2.12	1.52	1.12
	Ramp 3	1.19	0.75	0.89
Back top	Ramp 1	3.08	2.28	1.08
	Ramp 2	2.02	1.43	1.02
	Ramp 3	1.06	0.62	0.76
Front top	Ramp 1	3.52	2.63	1.52
	Ramp 2	2.43	1.74	1.43
	Ramp 3	1.37	0.84	1.07

*All values in terms of Deg/Min

configuration yields the most stable curve, with the lowest standard deviation, of 0.5711. The mean deviation is also at a higher level in this configuration, which is ideal. According to this analysis, the top front configuration will lead to fewer rejected parts than the other configurations tested.

Figure 12 shows time vs. temperature for the front-bottom configuration. There were three parts with 4 TCs loaded in the autoclave in each cycle. Different colors correspond to different parts. It is evident that the 4 TCs associated with part 2 (bottom red lines), come close to the minimum requirements according to the required specifications shown by dashed black lines. Although they appear to remain above the minimum ramp rate for the duration of the curing cycle, in Fig. 13, they fall below the specification for a significant portion of the cure cycle. The specification requires that the minimum

average ramp rate for any 10-min duration remain above 2 °F per minute from 130 to 190 °F. From 170 to 190 °F, both PTC21 and PTC22 remain below 2 °F/min, indicating a part that should be rejected.

The discontinuities in Fig. 13 show the uneven heating inside the autoclave, the larger the disconnect, the longer the duration between a given TC reaching the next temperature range, and the slowest TC reaching the same range. Ideally, there would be no discontinuities in this graph. It is also evident that none of the thermocouples approach the upper limit of the ramp rate. The ramp rates in Fig. 13 are averaged over 10-min periods.

After dissecting the data from each batch, it proved valuable to evaluate the separate ramp rate regions at each configuration. Averaging the MD between all 3 ramp regions would cause the loss of valuable information. We wanted to observe if the two parameters had independent effects on the mean deviation (MD) in ramp regions 1, 2, and 3. Table 5 shows a summary of the data for each ramp region. These are the values that were the input in Minitab according to the design explained earlier.

The results show that in region 1, when the rack is in the front position, the expected MD is at its maximum. The rack level has nearly zero levels of impact on the output. The Pareto and normal plot analysis show factor A (rack position) has a significant effect on the output. The interaction factor_A × factor_B (position × level) has no statistically significant effect. Factor B (rack level) has no effect on the MD in ramp region 1.

In ramp region 2, when the rack is in the front position, the expected MD would be at its maximum. The rack level has little impact on the effect of the output. In this case, factor A (rack position) does not have a statistically significant effect
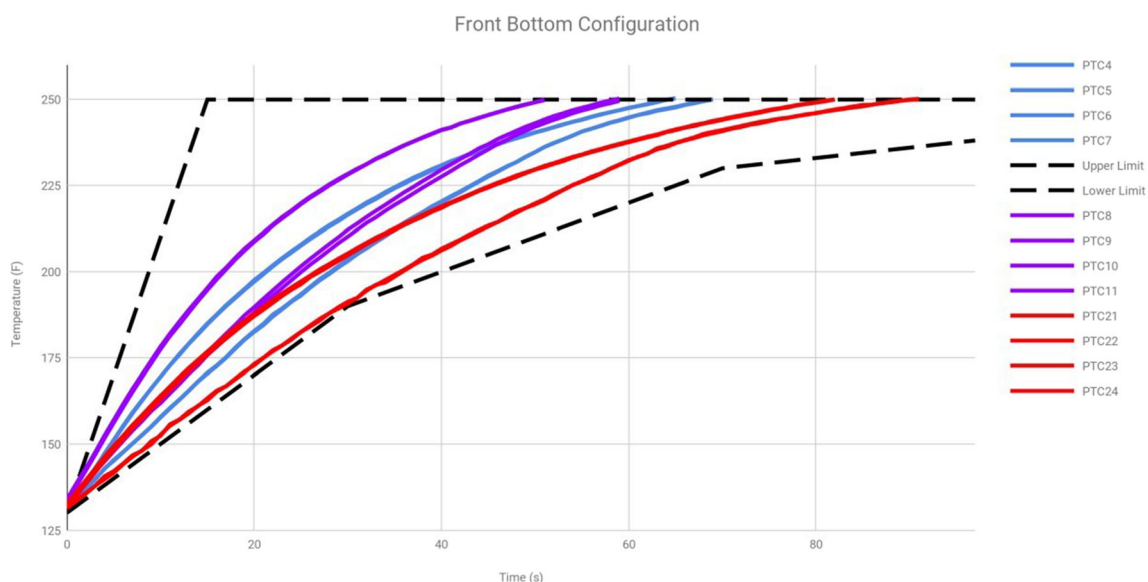

Fig. 12 Time vs. temp front-bottom front top purple, front bottom: blue, back bottom: red
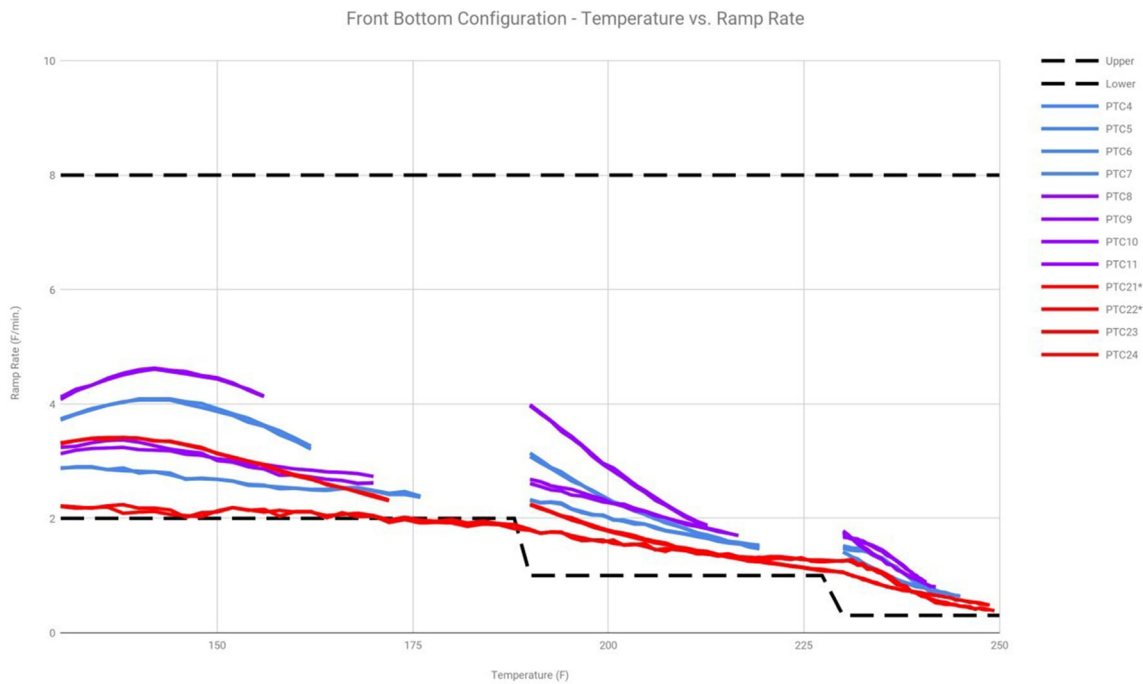
Fig. 13 Temp vs. ramp rate front-bottom

on the output but does have the highest effect among the 3 factors (A, B, and their interaction). The interaction factor A × factor B (position × level) and factor B (rack level) have small effects on the output but do not have statistically significant effects on the MD in ramp region 2.

In ramp region 3, results show when the rack is in the front position, the expected result is at its maximum. The rack level has little impact on the output. The interaction factor_A × factor_B (position × level), factor A (rack position), and factor B (rack level) are not statistically significant factors for the MD in ramp region 3.

4 Summary and recommendations

In the proposed study, we first used CFD simulation to investigate the effect of part location, direction, and quantity on the

Table 5 DOE test response values*

Configuration	MD-ramp 1	Mad-ramp2	MD-ramp3
Front bottom	1.46	1.38	1.01
Back bottom	1.14	1.12	0.89
Back top	1.08	1.02	0.76
Front top	1.52	1.43	1.07

*All values in terms of Deg/Min

heat transfer and curing cycle inside a model autoclave when a specific prism is used. The baseline model included 4 prims facing the autoclave front. The results showed that doubling the number of prims in the autoclave in two levels, without changing the direction of the molds, could impose a small lag in the heat-up portion of the curing cycle (~ 4 min) while the ramp-up rates are within the specifications. As a result, this loading of an autoclave will double the production rate in each cycle without comprising the quality of the parts or increasing the number of defective items.

We then experimentally investigated the effect of part location (front or back) and level (low or high rack) on the ramp-up rate of 3 parts provided by a partner company. The results of controlled experiments showed that loading parts in the front configuration lead to a statistically significant positive effect on the MD, while the rack position is not statistically significant. This result could verify the computational results obtained earlier that adding a new level will not have a significant impact on the quality of the parts.

In this paper, we explored the heat transfer during the heat-up portion of the curing cycle in an autoclave. Future works could involve modeling the full curing cycle from heat-up to cool-down and the conduction through the layers of the parts for a more accurate heat profile of the scenarios studied. We predict that there will be a lag in the cooling part of the curing cycle resulting from loading more parts similar to the heat-up section. As it is the same heat transfer process, in the opposite direction, the resulting lag will contribute to the total delay in the curing cycle.

Authors' contributions All authors contributed significantly to the work with the order provided.

Data availability Available in the "data deposition" file attached.

Compliance with ethical standards

Conflict of interest The authors declare that they have no conflict of interest.

Code availability Available in the "data deposition" file attached.

References

1. Lee S-Y, Springer GS (1988) Effects of cure on the mechanical properties of composites. J Compos Mater 22(1):15–29. https://doi.org/10.1177/002199838802200102

2. Peters PWM (1994) Influence of cure temperature and degree of surface treatment on transverse cracking and fibre/matrix bond strength in CFRP. J Compos Mater 28(6):507–525. https://doi.org/10.1177/002199839402800602

3. C. Gernaat, S. Alavi-Soltani, M. Guzman, A. Rodriguez, B. Minaie, and J. Welch, "Correlation between viscoelastic and mechanical properties for an out-of-autoclave polymer composite," 2009

4. Alavi-Soltani S, Sabzevari S, Koushyar H, Minaie B (2012) Thermal, rheological, and mechanical properties of a polymer composite cured at different isothermal cure temperatures. J Compos Mater 46(5):575–587. https://doi.org/10.1177/0021998311415443

5. Cao Y, Cameron J (2007) The effect of curing conditions on the properties of silica modified glass fiber reinforced epoxy composite. J Reinf Plast Compos 26(1):41–50. https://doi.org/10.1177/0731684407069950

6. White SR, Kim YK (1996) Staged curing of composite materials. Compos A: Appl Sci Manuf 27(3):219–227. https://doi.org/10.1016/1359-835X(95)00023-U

7. Bowles KJ, Frimpong S (1992) Void effects on the interlaminar shear strength of unidirectional graphite-fiber-reinforced composites. J Compos Mater 26(10):1487–1509. https://doi.org/10.1177/002199839202601006

8. Tang C, Li Y, Dong X, He B (2020) A generalized alternating linearization bundle method for structured convex optimization with inexact first-order oracles. Algorithms 13(4):Art. no. 4. https://doi.org/10.3390/a13040091

9. Boey FYC, Lye SW (1992) Void reduction in autoclave processing of thermoset composites: part 1: high pressure effects on void reduction. Composites 23(4):261–265. https://doi.org/10.1016/0010-4361(92)90186-X

10. Liu L, Zhang B-M, Wang D-F, Wu Z-J (2006) Effects of cure cycles on void content and mechanical properties of composite laminates. Compos Struct 73(3):303–309. https://doi.org/10.1016/j.compstruct.2005.02.001

11. Olivier P, Cottu JP, Ferret B (1995) Effects of cure cycle pressure and voids on some mechanical properties of carbon/epoxy laminates. Composites 26(7):509–515. https://doi.org/10.1016/0010-4361(95)96808-J

12. Boey FYC, Lye SW (1990) Effects of vacuum and pressure in an autoclave curing process for a thermosetting fibre-reinforced composite. J Mater Process Technol 23(2):121–131. https://doi.org/10.1016/0924-0136(90)90152-K

13. Guo Z-S, Liu L, Zhang B-M, Du S (2009) Critical void content for thermoset composite laminates. J Compos Mater 43(17):1775–1790. https://doi.org/10.1177/0021998306065289

14. Mouritz AP (2000) Ultrasonic and interlaminar properties of highly porous composites. J Compos Mater 34(3):218–239. https://doi.org/10.1177/002199830003400303

15. Müller De Almeida SF, Chaves De Mas Santacreu A (1995) Environmental effects in composite laminates with voids. Polym Polym Compos 3(3):193–204

16. Costa ML, Rezende MC, De Almeida SFM (2005) Strength of hygrothermally conditioned polymer composites with voids. J Compos Mater 39(21):1943–1961. https://doi.org/10.1177/0021998305051807

17. Koushyar H, Alavi-Soltani S, Minaie B, Violette M (2012) Effects of variation in autoclave pressure, temperature, and vacuum-application time on porosity and mechanical properties of a carbon fiber/epoxy composite. J Compos Mater 46(16):1985–2004. https://doi.org/10.1177/0021998311429618

18. Struzziero G, Skordos AA (2017) Multi-objective optimisation of the cure of thick components. Compos A: Appl Sci Manuf 93:126–136. https://doi.org/10.1016/j.compositesa.2016.11.014

19. Wang Q, Wang L, Zhu W, Xu Q, Ke Y (2017) Design optimization of molds for autoclave process of composite manufacturing. J Reinf Plast Compos 36(21):1564–1576. https://doi.org/10.1177/0731684417718265

20. Hu J, Zhan L, Yang X, Shen R, He J, Peng N (2020) Temperature optimization of mold for autoclave process of large composite manufacturing. J Phys Conf Ser 1549:032086. https://doi.org/10.1088/1742-6596/1549/3/032086

21. Kluge N, Lundström T, Ljung A-L, Westerberg L, Nyman T (2016) An experimental study of temperature distribution in an autoclave. J Reinf Plast Compos 35(7):566–578. https://doi.org/10.1177/0731684415624768

22. Bohne T, Frerich T, Jendrny J, Jürgens J-P, Ploshikhin V (2018) Simulation and validation of air flow and heat transfer in an autoclave process for definition of thermal boundary conditions during curing of composite parts. J Compos Mater 52(12):1677–1687. https://doi.org/10.1177/0021998317729210

23. Slesinger N, Shimizu T, Arafath ARA, Poursartip A Heat transfer coefficient distribution inside an autoclave:10

24. Sturrock NS (1971) Localized boundary-layer heat transfer from external building surfaces. PhD Thesis, University of Liverpool

25. Rowley FB, Eckley WA (1932) Surface coefficients as affected by wind direction. ASHRAE Trans 38:33–46

Publisher's note Springer Nature remains neutral with regard to jurisdictional claims in published maps and institutional affiliations.